Using Local Binary Patterns in Speckle Image Analysis

L. Bento[1], L. Távora[2], P. Assunção[1,2], S. Faria[1,2] and R. Fonseca-Pinto[1,2]
[1] Instituto de Telecomunicações, Multimedia Signal Processing, Leiria, Portugal
[2] Polytechnic Institute of Leiria, Leiria, Portugal
rui.pinto@ipleiria.pt

Abstract - **Firstly described by Newton in the 17th century, speckle is an optical phenomenon which can be translated into image patterns produced by wave interferences of diffused reflections. In fact, the speckle pattern is generated by the multiple interference phenomena that occur when a rough surface is illuminated with a coherent source of light, producing randomly distributed reflected waves of the same frequency but different phases and amplitudes. Although it has been known for a long time, capturing video sequences of speckle patterns was dependent on recent technological developments, in particular, related to laser technology and microsensors. The speckle acquisition setup comprises a light source, usually a laser, an optical beam expander and a CCD camera. The generated interference patterns are captured in series of video sequences, to further be processed. In previous works, several image processing algorithms have been applied to analyze video frames of speckle, aimed to capture the evolution patterns in dynamic processes. However, due to the typical high frequencies of the changing patterns, classical texture algorithms mostly fail this goal. In this work, speckle dynamics are evaluated using Local Binary Patterns (LBP) jointly with some of its main variants and a newly proposed algorithm, in a reactive hyperemia controlled test. The proposed methodology goes beyond the traditional implementations of LBPs, by considering an additional Gaussian filtering, a methodology thus coined as LBPg. The results, on one hand, confirm that the classical formulations of LBP are not sensitive to changes in the simulated patterns but, on the other hand, demonstrate that the newly proposed LBP-adapted algorithm successfully identify the dynamics of the processes under study.**

Keywords – Local Binary Patterns; Laser Speckle; Video Processing; Computer Vision.

I. INTRODUCTION

Speckle imaging is an optical intensity pattern produced by mutual interference of wavefronts scattered from a rough surface [1]. Whenever a coherent light source interacts with a medium, the surface geometry (static or dynamic) induces phase shifts in the scattered light, producing constructive or destructive interference. The temporal and spatial statistics of the varying pattern that is produced provides information about the motion of the scattering particles [2]. Although the physical phenomenon has already been described by Newton, the theory only gained a strong impulse in the 1960's and following of the last century, allied to the technological development of lasers and optical sensors.

When lasers were invented, the speckle effect was initially seen as a major limitation upon object illumination. In fact, in holographic imaging and in laser-based display systems (e.g. Laser TV) the speckle contrast reduction is highly desirable once as it tends to mask the image information [3]. Later on, it was proved that the granular effect was strongly correlated with the characteristics of the surface, either when a static surface is illuminated or when a dynamic process underneath the surface tends to deform the surface itself (i.e. by some type of motion). Accordingly, the so far artifact, became a useful feature to exploit in different scientific contexts and objectives, ranging from material sciences to medical applications.

The motion of the scattering induces front-wave interference, which will be further captured by a digital sensor in terms of pixel intensities, ranging from dark to white in a grayscale image. This type of changing pattern can be quantified through the image processing of the obtained grayscale images using spatial [4] or temporal statistics measures [5], spatiotemporal algorithms, or frequency derived algorithms [6]. Recently, unsupervised machine learning algorithms have been applied in the characterization of dynamic speckles to identify regions with the same activity pattern [7, 8].

The objective of this work is to present a comparison of methods based on Local Binary Patterns – LBP, when applied in laser speckle video processing. This comparison includes the results of LBP_g, recently proposed by our group to characterize skin perfusion profiles.

In the remainder of this paper, in Section II the methodology is presented and in Section III, the obtained results are shown. Section IV is dedicated to discussion and finally, in Section V, the conclusions are presented.

II. METHODOLOGY

A. Local Binary Pattern Algorithms

The LBP was first proposed in [9] as a 2D texture operator by integrating the local variations of the spatial pattern with a grayscale coding scheme. This method proved to be of easy implementation, invariant to

[1] This work was supported by Fundação para a Ciência e Tecnologia FCT- Portugal, under the scope of Light Field Laser Speckle project in the scope of R&D Unit 50008, through national funds and where applicable co-funded by FEDER - PT2020 partnership agreement

monotonic illumination and having low computational complexity [10].

The LBP code of a given pixel is defined in (1);

$$LBP = \sum_{p=0}^{7} s(I_P - I_C)2^p, \quad s(x) = \begin{cases} 1 \; if \; x \geq 0 \\ 0 \; if \; x < 0 \end{cases} \qquad (1)$$

where I_p and I_C are, respectively, the intensity of the peripheral and central pixels and P de number of neighboring points. The definition can be generalized to a given radius R and a number of points P, as illustrated in Figure 1.

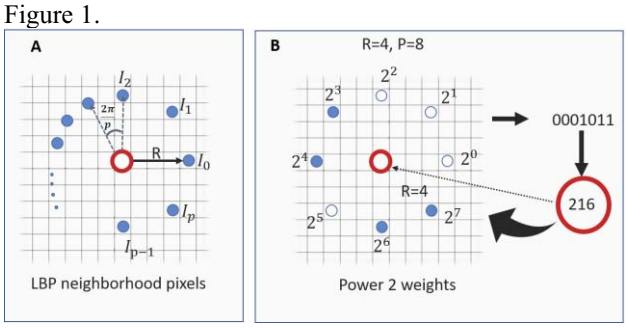

Figure 1: General LBP overview: A-neighborhood pixel geometry, B-LBP example using R=4 and P=8.

The original definition (1) has several variants, that have been proposed to overcome the identified issues when it is applied with distinct research purposes. In particular, LBP has limitations in detect large-scale textural structures and is sensitive to image rotation. Moreover, the methodology applies a fixed and coarse quantization using the sign of the differences between neighboring pixels thus being highly sensitive to noise [10].

The Local Binary Standard (CLBP) decomposes local differences into two complementary components: the signal (calculated in (1)) and magnitude (2);

$$CLBP_M = \sum_{p=0}^{7} f_2(|I_p - I_c|, T_{\Delta\bar{I}})2^p, f_2 = \begin{cases} 1, x \geq T_{\Delta\bar{I}} \\ 0, x < T_{\Delta\bar{I}} \end{cases} \quad (2)$$

where, $T_{\Delta\bar{I}}$ is the average value of the difference in grey value between a pixel in the periphery and the central pixel. In addition to these two components, the CLBP also includes image intensity information:

$$CLBP_C = f_2(I_c, \bar{T}_I) \qquad (3)$$

where f_2 was previously defined in (2) and the threshold $\bar{T}_I$ is set as the average gray level of the whole image. The three code maps are combined to form the CLBP final histogram that allows characterizing the texture [11].

The local binary patterns in three orthogonal planes (LBP-TOP) is a spatiotemporal variant of the canonical LBP operator that allows to combine movement and appearance. LBP-TOP considers three orthogonal planes: XY, XT and YT and concatenates the local statistics of co-occurrence of binary patterns in these three directions. The final histogram of the LBP-TOP can be defined as:

$$H_{i,j} = \sum_{x,y,t} I\{f_j(x,y,t) = i\}, i = 0, \ldots, n_{j-1}; j = 0,1,2 \quad (4)$$

in which n_j is the number of different labels produced by the LBP operator in the j^{th}, $f_i(x,y,t)$ expresses the LBP code of central pixel (x,y,t) in the j^{th} plane, and

$$I\{A\} = \begin{cases} 1, & if \; A \; is \; true \\ 0, & if \; A \; is \; false \end{cases}$$

When the features to be compared are of different spatial and temporal sizes, the histograms must be normalized [12].

Regarding the multi-quantified local binary pattern scheme (MQLBP), it allows quantifying the gray level difference at a desirable number of levels (N), using a threshold parameter γ. Each level is quantified according to the function f_n, defined as:

$$f_n(x,y) = \begin{cases} 0, x < -(N-1)\gamma \\ 1, (N-1)\gamma \leq x < -(N-2)\gamma \\ \vdots \\ N-1, -\gamma \leq x < 0 \\ N, 0 \leq x < \gamma \\ N+1, \gamma \leq x < 2\gamma \\ \vdots \\ 2N-2, (N-2)\gamma \leq x < (N-1)\gamma \\ 2N-1, x \geq (N-1)\gamma \end{cases} \qquad (5)$$

producing $2N$ segments and the MQLBP code, corresponding to the i^{th} segment is calculated as follows:

$$MQLBP^i = \sum_{p=0}^{P-1} \delta(f_N(I_p - I_c, \gamma) - i)2^p, \qquad (6)$$

$$\delta(x) = \begin{cases} 1, & x = 0 \\ 0, & otherwise \end{cases}$$

The final histogram to characterize the texture results from the concatenation of the calculated histograms for each of the segments [13].

In (1) the gradient to the central pixel is not considered, but his signal. To overcome this constraint, the LBPg is also proposed in this work, whose definition for each pixel is presented in (7).

$$LBP = \sum_{P=0}^{7} s[g(I_P - I_C)]2^P \qquad (7)$$

where I_P and I_C are respectively the intensity of the peripheral and central pixels, s is a step function defined in (8) and g the Gaussian function.

$$s(x) = \begin{cases} 1 & if x \in FWHM_{g_{(\mu,\sigma)}} \\ 0, & otherwise \end{cases} \qquad (8)$$

where $\mu_{\bar{x}}$ and $\sigma_{\bar{x}}$ are respectively, the average and standard deviation of the absolute differences to the central pixel in a 3×3 neighborhood.

To obtain a relative measure of the activity a basal video sequence was selected (B) to further compare with the activity in other time intervals (S). To compare the dynamic patterns, four metrics relating the histograms of each video sequence H_B and H_S were implemented. These metrics (Chi-square - χ^2, Correlation - C, Intersection - I and Euclidian distance - E_d) were aplied to the normalized histograms H_B, and H_S as defined in (9).

B. Instrumentation and Experimental Protocols

For the purpose of this work, an acquisition setup was built, composed by a class III laser beam (633×10^{-9} m

wavelength and 5 mW Power). A beam expander and a CCD Camera (Sony, nxcam AVCHD, 50 fps) were also integrated into the setup as illustrated in Figure 2.

$$\chi^2 = \sum_i \frac{(H_B(i) - H_S(i))^2}{(H_B(i) + H_S(i))};$$

$$C = \frac{\sum_i (H_B(i) - \overline{H_B})(H_S(i) - \overline{H_S})}{\sqrt{\sum_i (H_B(i) - \overline{H_B})^2 \sum_i (H_S(i) - \overline{H_S})^2}}$$

$$I = \sum_i \min(H_B(i), H_S(i)) \quad (9)$$

$$E_d = \sqrt{\sum_{i=0} (H_B(i) - H_S(i))^2}$$

where, $\overline{H_k} = \frac{\sum_i (H_k(i))}{N}$ and N is the number of bins in the histograms.

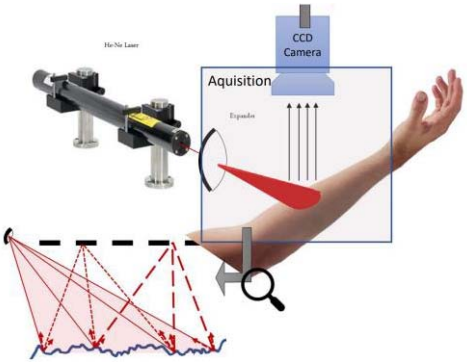

Figure 2 Acquisition Setup.

In order to compare the five LBP derived methodologies in distinct speckle dynamic patterns, an experimental protocol of skin microcirculation simulating hypoxia followed by perfusion (occlusion hyperemia test - OHT) was conducted in distinct ROIs at the upper limb. The OHT was performed in a controlled environment, in which the volunteers stay in a seated position for 5 minutes prior to the test. For each subject, distinct ROIs at the forearm and hand (dorsal and ventral) were tested in distinct perfusion conditions (basal, occlusion and hyperemia). The occlusion was simulated using a cuff pressure at the arm, inflated at 160 mmHg, during an occlusion interval of 60 seconds, followed by hyperemia and returning to basal conditions.

III. Results and Discussion

The perfusion profiles obtained during OHT for each LBP derived methodology and for each metric defined in (4) are presented in Figure 3. The opening instants of the cuff-pressure valve (i.e. the instants when the perfusion is restored) are marked with a vertical bar. This bar delimits the occlusion region, which is anterior, followed by a rapid increase of perfusion (i.e. hyperemia) and the return to basal conditions.

To test the consistency of the findings, additional tests were performed in which the perfusion profile was evaluated in different ROIs of the same volunteer under the same perfusion conditions. In this case, data was obtained from two regions of the hand (dorsal and ventral) in two volunteers (V1 and V2), as shown in Figure 4. In this case, the chosen metric for histogram caparison was the χ^2 metric.

The processing of speckle video frames is a challenging task. The type of features joint with their difficult perception to the human eye (even when the assessed phenomena have high-intensity variation) make it difficult to choose the image processing technique to be used as first choice. The patterns and textures that are perceived tend to put spatial methods of local analysis as a primary choice. Nonetheless, the results presented in this work clearly indicate the failure of the classical LBP method to detect dynamic changes in the speckle pattern (particularly in identifying the perfusion changes induced by the OHT). This result can be observed in the first column of Figure 3 for all the metrics used in this work, in which the perfusion pattern is slightly constant (even after the release of the cuff-pressure denoted by the vertical bar in Figure 3).

The CLBP methodology put forward a strategy to use the intensity gradient to the central pixel (instead of simply using the signal itself), preserving the information about local structures to be analyzed. Nevertheless, the results of CLBP in the OHT show rather limited sensitivity to identify the transition to the greatest activity period. It is interesting to note that in the case of E_d, when compared with χ^2 metric, the sensitivity is greatly reduced although the similarity of the definition (both are based on the difference of histograms, however the χ^2 metric is a normalized result).

The LBP-TOP is a simplified version of the Volume-LBP (built in terms of a cube of textons) aimed to capture the spatiotemporal dynamics in three orthogonal plans. According to the results in column 3 of Figure 3, the instants were the perfusion profile is changing are clearly identified, however it is possible to verify that (regardless of the applied metric) the LBP-TOP only identifies those where there is a high gradient in the activity. Regarding the analysis of MQLBP and the associated metrics, it is possible to verify the matching of the χ^2 and E_d derived profiles with the perfusion levels imposed by the experimental OHT protocol.

The LBP_g methodology, due to the combined ability to capture the differences between neighboring pixels and the local filtering approach (implemented through the Gaussian thresholding), allows an efficient characterization of speckle activity profiles. This methodology proved to be effective in identifying the instants where the perfusion profile is altered, regardless of the applied metric.

In what concerns the methodologies that proved to be sensitive to the changing of the perfusion patterns, the χ^2 metric is the one presenting consistent results, thus it was applied in the remaining tests. To test ROI texture dependence in LBP_g+χ^2 methodology, several perfusion profiles were experimentally simulated by OHT and measured at the hand. The results for the dorsal and ventral regions in two volunteers are shown in Figure 4. The perfusion profile allows to conclude that ROI texture has

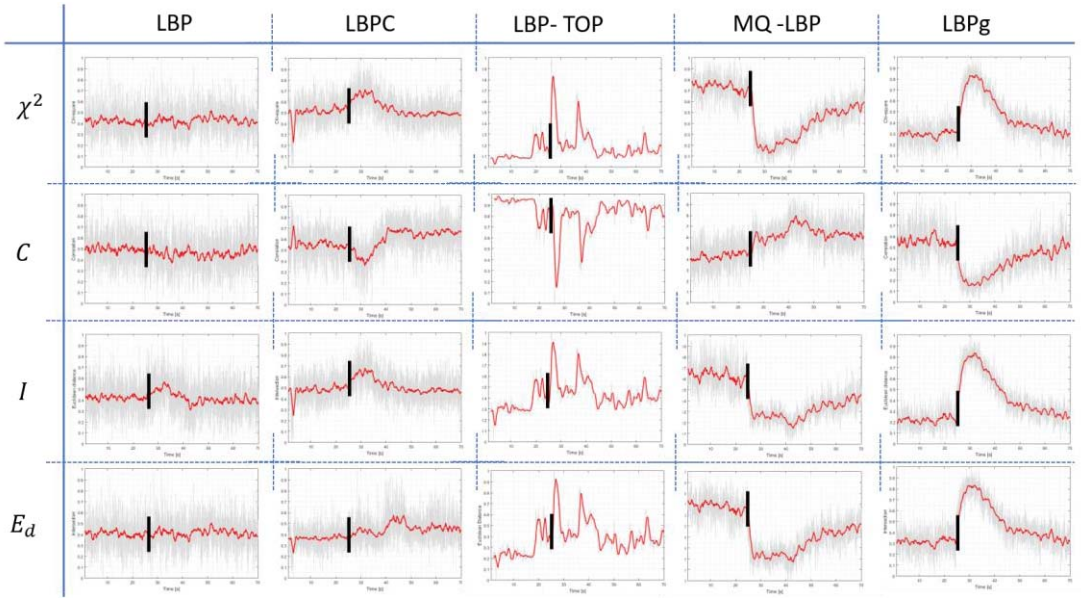

Figure 3: Perfusion profiles in OHT using LBPs methodologies and four metrics. The time of cuff release pressure is marked with a vertical bar

no significant influence on the identification of the perfusion trend.

Moreover, in the ventral region (due to the proximity of large vessels) the changes in the perfusion profiles were in fact highlighted on both cases. The results reported in this work clearly point out to the use a relative measure based on the suggested $LBP_g+\chi^2$ algorithm in Laser Speckle Imaging studies of skin perfusion. Indeed, the methodology proved to be sensitive to the changing of the perfusion profile and rather independend of the skin ROI texture.

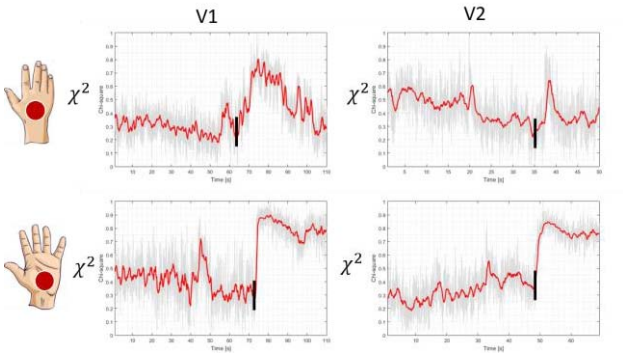

Figure 4: Qui-squared LBPg metric for dorsal (first row) and ventral (second row) perfusion profiles for two volunteers (V1 and V2)

IV. Conclusion

This work reports a comparative study of video speckle processing techniques based on LBP and some of its classical derivations. In particular, a new technique based on a Gaussian filtering was also tested, the LBP_g. Dynamic Speckle profiles were assessed by simulating upper limb perfusion conditions using the OHT test. Amongst the tested methodologies, the LBP_g proved to be sensitive to the changing of perfusion levels for any of the tested metrics.

To assess the influence of ROI texture on the perfusion results, different regions with the same perfusion profile were tested. The results show that the $LBP_g + \chi^2$ methodology is appropriate to identify perfusion changes regardless of the ROI texture.

The comparison results of LBP techniques allows concluding that classic aproach is not suitable for video speckle analysis. However, specific variations on the original methodology (which target the characteristics of the speckle images) allows us to obtain a low computational, noise sensitive methodology to track dynamic speckle activity.

V. References

[1] C. Dainty, Laser Speckle and Related Phenomena, Sprinter Verlag, 1984.

[2] D. A. Boas e A. K. Dunn, "Laser speckle contrast imaging in biomedical optics," *Journal of Biomedical Optics, 15 (1),* p. 011109, 2010.

[3] J. W. Goodman e J. I. Trisnadi, "Speckle Reduction by a Moving Diffuser in Laser Projection Displays," em *Annual Meeting of the Optical Society of America*, Rhode Island, 2000.

[4] A. F. Fercher e J. D. Briers, "Flow visualization by means of single-exposure speckle photography," *Opt. Commun,* vol. 37, pp. 326-330, 1981.

[5] K. R. Forrester, J. Tulip, C. Leonard, C. Stewart e R. C. Bray, "A laser speckle imaging technique for measuring tissue perfusion.," *IEEE Trans Biomed Eng,* vol. 51(11), pp. 2074-84., 2004.

[6] H. J. Rabal e R. A. Braga, Dynamic Laser Speckle and Applications, CRC Press, 2008.

[7] G. Meschino, S. Murialdo, I. Passoni, H. J. Rabal e M. Trivi, "Biospeckle image stack process based on artificial neural networks," *Proceedings of the Engineering in Medicine and Biology Society,* pp. 4056-4059, 2010.

[8] L. Bento, L. Távora, P. Assunção, S. Faria e R. Fonseca-Pinto, "Dynamic Laser Speckle in Medical Imaging: On the quantification of skin patterns," em *Proceedings of the New Health Researchers 2016*, 2017.

[9] T. Ojala, M. Pietikäinen e D. Harwood, "A Comparative Study of Texture Measures with Classification Based on Feature Distributions," *Pattern Recognition,* vol. 19 (3), pp. 51-59, 1996.

[10] L. Liu, P. Fieguth, Y. Guo, X. Wang e M. Pietikäinen, "Local Binary Features for Texture Classification: Taxonomy and Experimental Study," *Pattern Recognition,* vol. 62, pp. 135-160, 2017.

[11] Guo, Zhenhua, L. Zhang e D. Zhang, "A Completed Modeling of Local Binary Pattern Operator for Texture Classification," *IEEE Transactions on Image Processing,* vol. 19, nº 6, pp. 1657 - 1663, 2010.

[12] G. Zhao e M. Pietikäinen, "Dynamic texture recognition using local binary patterns with an application to facial expressions," *IEEE Transactions on Pattern Analysis and Machine Intelligence,* vol. 29, nº 6, pp. 915 - 928, 2007.

[13] B. Patel, R. Maheshwari e R. Balasubramanian, "Multi-quantized local binary patterns for facial gender classification," *Computers & Electrical Engineering,* vol. 54, nº C, pp. 271-284, 2016.